

## Crystal Structure and Physical Properties of a New $\text{CuTi}_2\text{S}_4$ Modification in Comparison to the Thiospinel

Navid Soheilnia,<sup>†</sup> Katja M. Kleinke,<sup>†</sup> Enkhtsetseg Dashjav,<sup>†</sup> Heather L. Cuthbert,<sup>‡</sup> John E. Greedan,<sup>‡</sup> and Holger Kleinke<sup>\*†</sup>

Department of Chemistry, University of Waterloo, Waterloo, ON, Canada N2L 3G1, and Department of Chemistry and the Brockhouse Institute for Materials Research, McMaster University, Hamilton, ON, Canada L8S 4M1

Received April 14, 2004

A new modification of  $\text{CuTi}_2\text{S}_4$  was prepared from the elements at 425 °C. It crystallizes in the rhombohedral space group  $R\bar{3}m$ , with lattice parameters of  $a = 7.0242(4)$  Å,  $c = 34.834(4)$  Å, and  $V = 1488.4(2)$  Å<sup>3</sup> ( $Z = 12$ ). Two topologically different interlayer regions exist between the close-packed S layers that alternate along the  $c$  axis: one comprises both Cu (in tetrahedral voids) and Ti atoms (in octahedral voids), and the second exclusively Ti atoms (again in octahedral voids). In contrast to the known modification, the spinel, Cu–Ti interactions of 2.88 Å occur that have bonding character according to the electronic structure calculations. Both  $\text{CuTi}_2\text{S}_4$  modifications are metallic Pauli paramagnets due to Ti d contributions. The Pauli susceptibility of the  $R\bar{3}m$  form is larger than that of the thiospinel in quantitative agreement with the LMTO-ASA band structure calculations. The irreversible transformation to the spinel takes place at temperatures above 450 °C.

### Introduction

Several copper-containing thiospinels have attracted wide interest as a consequence of their unusual physical properties. Many studies on different properties were performed, e.g. on ferro-<sup>1</sup> and antiferromagnetism,<sup>2</sup> superconductivity,<sup>3–5</sup> spin-glass transitions,<sup>6</sup> and thermoelectric properties.<sup>7</sup> In the past, thiospinels were also under investigation as cathodes for secondary lithium batteries during the 1980s and -90s.<sup>8</sup> Among the most studied Cu thiospinels is (doped)  $\text{CuIr}_2\text{S}_4$

that shows an interesting metal–nonmetal transition<sup>9–12</sup> with a rare simultaneous charge ordering and spin dimerization transition.<sup>13</sup>

The cubic thiospinel  $\text{CuTi}_2\text{S}_4$  was structurally characterized a long time ago.<sup>14</sup> To date, the investigations of its physical properties remain to be inconclusive, which may in part be due to the tendency to be Cu-deficient.<sup>15,16</sup> Half-metallic ferromagnetism was predicted from band structure calculations,<sup>17</sup> while experimental reports indicated either a spin gap at 5 K<sup>18</sup> or a more conventional Pauli paramagnetism.<sup>19</sup> Our attempts to grow single crystals of  $\text{CuTi}_2\text{S}_4$  using a KCl/

\* Author to whom correspondence should be addressed. E-mail: kleinke@uwaterloo.ca.

<sup>†</sup> University of Waterloo.

<sup>‡</sup> McMaster University.

- (1) Endoh, R.; Awaka, J.; Nagata, S. *Phys. Rev.* **2003**, *B68*, 115106/115101–115106/115109.
- (2) Miyatani, K.; Tanaka, T.; Ishikawa, M. *J. Appl. Phys.* **1998**, *83*, 6792–6794.
- (3) Van Maaren, M. H.; Schaeffer, G. M.; Lotgering, F. K. *Phys. Lett.* **1967**, *A25*, 238–239.
- (4) Goto, A.; Shimizu, T.; Cao, G.; Suzuki, H.; Kitazawa, H.; Matsumoto, T. *Physica* **2000**, *C341–348*, 737–738.
- (5) Cao, G.; Furubayashi, T.; Suzuki, H.; Kitazawa, H.; Matsumoto, T.; Uwatoko, Y. *Phys. Rev.* **2001**, *B64*, 214514/214511–214514/214510.
- (6) Goya, G. F.; Rechenberg, H. R.; Sagredo, V. *J. Magn. Magn. Mater.* **2001**, *226–230*, 1298–1299.
- (7) Balcerek, K.; Marucha, C.; Wawryk, R.; Tyc, T. *Philos. Mag.* **1999**, *B79*, 1021–1028.
- (8) Imanishi, N.; Inoue, K.; Takeda, Y.; Yamamoto, O. *J. Power Sources* **1993**, *44*, 619–625.

- (9) Nagata, S.; Matsumoto, N.; Kato, Y.; Furubayashi, T.; Matsumoto, T.; Sanchez, J. P.; Vulliet, P. *Phys. Rev.* **1998**, *B58*, 6844–6854.
- (10) Endoh, R.; Matsumoto, N.; Chikazawa, S.; Nagata, S.; Furubayashi, T.; Matsumoto, T. *Phys. Rev.* **2001**, *B64*, 075106/075101–075106/075107.
- (11) Endoh, R.; Matsumoto, N.; Awaka, J.; Ebisu, S.; Nagata, S. *J. Phys. Chem. Solids* **2002**, *63*, 669–674.
- (12) Nagata, S.; Ito, S.; Endoh, R.; Awaka, J. *Philos. Mag.* **2002**, *B82*, 1679–1694.
- (13) Radaelli, P. G.; Horibe, Y.; Gutmann, M. J.; Ishibashi, H.; Chen, C. H.; Ibberson, R. M.; Koyama, Y.; Hor, Y.-S.; Kiryukhin, V.; Cheong, S.-W. *Nature (London)* **2002**, *416*, 155–158.
- (14) Hahn, H.; Harder, B. *Z. Anorg. Allg. Chem.* **1956**, *288*, 257–259.
- (15) James, A. C. W. P.; Goodenough, J. B.; Clayden, N. J.; Banks, P. M. *Mater. Res. Bull.* **1989**, *24*, 143–155.
- (16) Kusawake, T. T.; Y.; Wey, M. Y.; Ohshima, K.-I. *J. Phys.: Condens. Matter* **2001**, *13*, 9913–9921.
- (17) Park, M. S.; Kwon, S. K.; Min, B. I. *Phys. Rev.* **2001**, *B64*, 100403/100401–100403/100404.

KI flux uncovered a new kinetically stabilized, rhombohedral modification of  $\text{CuTi}_2\text{S}_4$ . This article deals with its structural and physical properties in comparison to the spinel modification.

## Experimental Section

**Synthesis.** All reactions were carried out in evacuated sealed silica tubes starting from the elements with nominal purities above 99.5%, used as acquired from Aldrich or Alfa Aesar. We discovered the rhombohedral variant of  $\text{CuTi}_2\text{S}_4$  after heating a mixture of Cu, Ti, and S with an excess 1:1 mixture of KCl/KI (Ti:K ratio of 1:2) to 750 °C, followed by slow cooling to room temperature over a period of 1 week. Phase-pure rhombohedral  $\text{CuTi}_2\text{S}_4$  was obtained by annealing the elements in the stoichiometric 1:2:4 ratio at 425 °C over a period of 4 weeks, interrupted midway for grinding to increase homogeneity. Similarly, we prepared phase-pure cubic  $\text{CuTi}_2\text{S}_4$  within 1 week by annealing at 700 °C starting from the elements in the same stoichiometric ratio.

Reaction temperatures intermediate between 450 and 600 °C resulted in mixtures of both modifications within the time periods investigated, from a few days to 2 weeks. The transformation is a slow process at intermediate temperatures: after 1 week at 500 °C the reaction mixture contained both modifications in comparable amounts, while 1 week at 700 °C led to a complete transformation to the spinel. Shorter heating at temperatures above 500 °C, followed by long annealing at 425 °C, did not result in phase-pure formation of the rhombohedral variant. This indicates that the spinel, once formed, cannot be transformed into the rhombohedral form under thermodynamically controlled conditions. On the other hand, annealing the rhombohedral form at 700 °C followed by slow cooling without adding a flux agent yielded complete formation of the thiospinel.

To summarize, the cubic thiospinel  $\text{CuTi}_2\text{S}_4$  can be prepared directly from the elements at annealing temperatures of at least between 500 and 700 °C, while the rhombohedral form can only be obtained at temperatures between 380 and 450 °C, unless a flux such as KCl/KI is added. Then, the rhombohedral modification nucleates first during the cooling process. (Below 380 °C, only binaries formed.) Hence, the cubic form is thermodynamically preferred over the rhombohedral form over a wide temperature range, which in turn is the kinetically stabilized variant. It is not uncommon to find kinetically stabilized modifications during the cooling process when using a flux.<sup>20</sup>

**Analyses.** Phase identifications were carried out by powder X-ray diffractometry (using an INEL diffractometer with position-sensitive detector and Cu  $\text{K}\alpha_1$  radiation) from the ground products in all cases. Selected crystals were analyzed by means of standardless energy dispersive spectroscopy (EDS, LEO 1530, with integrated EDAX Pegasus 1200) using an acceleration voltage of 21 kV. In either case, the spectrum was comprised solely of the peaks characteristic for Cu, Ti, and S. It is concluded that no impurities, which might have come from the silica tube (silicon, oxygen) or the flux agent (K, Cl, I), were incorporated. Semiquantitative results were obtained by integrating over the  $\text{K}\alpha$  peaks of Cu (at 8.040 keV), Ti (4.508 keV), and S (2.307 keV). This resulted in comparable Cu:Ti:S ratios in both cases, namely 20:26:55 (in at. %) for the rhombohedral form and 18:27:55 for the cubic form.

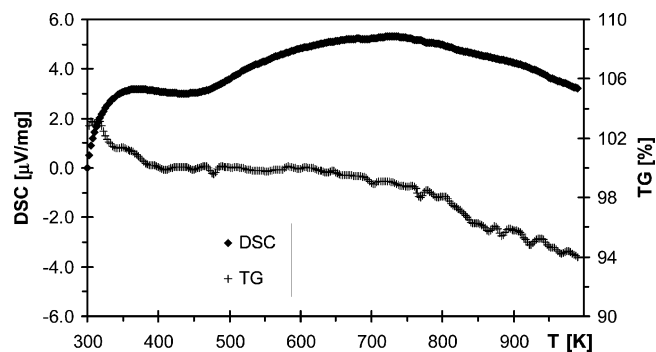


**Figure 1.** DSC and TG curves of rhombohedral  $\text{CuTi}_2\text{S}_4$  measured under a flow of argon.

Overall, this is in reasonable agreement with the ratio calculated from the formula  $\text{CuTi}_2\text{S}_4$  (14:29:57), noting that the Cu contents were clearly overestimated in both EDS analyses. To clarify whether the latter is a basic rule for the current machine setup, we analyzed the binary monosulfide CuS as well. The obtained values of 58(1):42 at. % (instead of the ideal 50:50 ratio) confirmed the suspected trend that the Cu:S ratio is generally too high in these EDS analyses.

Next, a temperature-dependent combined differential scanning calorimetry (DSC) and thermogravimetry (TG) measurement with the computer-controlled NETZSCH STA 409PC Luxx was performed between room temperature and 720 °C, starting from the rhombohedral modification. The measurement was carried out under a constant flow of argon (40 mL/min), which also protected the balance (flow of 30 mL/min). The heating rate was 20 °C/min. Because the phase transformation, starting between 450 and 500 °C, is a slow process below 600 °C, as revealed via different furnace experiments, no peaks in the DSC curve were expected and none were found (Figure 1). An X-ray powder diagram taken after this measurement revealed that the transformation to the cubic spinel took place. The rhombohedral form completely disappeared, and the spinel is the major product besides  $\text{Cu}_x\text{Ti}_2\text{S}_4$  with  $x < 0.3$  (revealed via X-ray powder diffraction and additional EDS analysis). The total weight loss of about 6%, apparently mainly Cu, inhibits 100% yield of the spinel.

A second DSC measurement was performed up to 600 °C, which yielded only small amounts of the spinel, with the major phase still being the rhombohedral modification. Of course, again no peak became visible in the DSC curve, since the transformation is expected to start below 500 °C, and it remained largely incomplete during the DSC experiment up to 600 °C.

**Single-Crystal Structures.** A black platelike crystal of the dimensions  $50 \times 35 \times 30 \mu\text{m}$  was selected for the structure determination of the rhombohedral form, and a black blocklike crystal ( $40 \times 33 \times 30 \mu\text{m}$ ) for a redetermination of the spinel form, to verify the Cu occupancy of the tetrahedral holes. The data collections were carried out on a Bruker Smart Apex CCD at room temperature utilizing Mo  $\text{K}\alpha$  radiation. Data were collected by scans of  $0.3^\circ$  in  $\omega$  at  $\phi = 0^\circ$  for an overall of 606 frames, with an exposure time of 60 s/frame in both cases. The data were corrected for Lorentz and polarization effects, and absorption corrections were based on fitting a function to the empirical transmission surface as sampled by multiple equivalent measurements.<sup>21</sup>

In the spinel case, we used the known atomic parameters and space group  $Fd\bar{3}m$ , starting with Cu on the tetrahedral and Ti on the octahedral sites. The structure refinements<sup>22</sup> converged to good

(18) Koyama, T.; Sugita, H.; Wada, S.; Miyatani, K.; Tanaka, T.; Ishikawa, M. *Physica* **2000**, *B284–288*, 1513–1514.

(19) Matsumoto, N.; Hagino, T.; Taniguchi, K.; Chikazawa, S.; Nagata, S. *Physica* **2000**, *B284–288*, 1978–1979.

(20) Hwang, S.-J.; Iyer, R. G.; Trikalitis, P. N.; Ogden, A. G.; Kanatzidis, M. G. *Inorg. Chem.* **2004**, *43*, 2237–2239.

(21) *SAINT*, version 4 ed.; Siemens Analytical X-ray Instruments Inc.: Madison, WI, 1995.

**Table 1.** Crystallographic Data for Cubic and Rhombohedral CuTi<sub>2</sub>S<sub>4</sub>

	cubic form	rhombohedral form
chem formula	CuTi <sub>2</sub> S <sub>4</sub>	CuTi <sub>2</sub> S <sub>4</sub>
fw	287.58	287.58
<i>T</i> of measmt (K)	293(2)	293(2)
$\lambda$ (Å)	0.710 73	0.710 73
space group	Fd $\bar{3}m$	R $\bar{3}m$
<i>a</i> (Å)	10.0059(7)	7.0242(4)
<i>c</i> (Å)		34.834(4)
<i>V</i> (Å <sup>3</sup> )	1001.8(1)	1488.4(2)
<i>Z</i>	8	12
$\mu$ (cm <sup>-1</sup> )	88.07	88.91
$\rho_{\text{calcd}}$ (g/cm <sup>3</sup> )	3.814	3.850
$R(F_o^a)/R_w(F_o^2)^b$	0.021/0.055	0.032/0.066

$${}^a R(F_o) = \frac{\sum ||F_o| - |F_c||}{\sum |F_o|}, {}^b R_w(F_o^2) = \frac{[\sum (w(F_o^2 - F_c^2)^2)]^{1/2}}{\sum [w(F_o^2)^2]^{1/2}}$$

**Table 2.** Atomic Positions and Isotropic Displacement Factors for Cubic CuTi<sub>2</sub>S<sub>4</sub>

atom	site	x	y	z	$U_{\text{eq}}/\text{Å}^2$
Cu	8 <i>a</i>	1/8	1/8	1/8	0.0125(2)
Ti	16 <i>d</i>	1/2	1/2	1/2	0.0116(2)
S	32 <i>e</i>	0.255 25(4)	0.255 25(4)	0.255 25(4)	0.0095(2)

residual values (e.g.,  $R(F) = 0.021$ ). Refining the occupancy factors of Cu and subsequently of Ti revealed no deficiencies or mixed occupancies.

In the case of the new, rhombohedral modification, the direct methods were employed in the centrosymmetric space group  $R\bar{3}m$ . All (nine) atomic positions were directly found, and their assignments were straightforward, based on both their peak heights and interatomic distances. The refinement converged to  $R(F) = 0.032$ . Again, we refined the occupancies of the Cu sites to check for deficiencies but found none. Then, we turned our attention to the Ti sites, noting that Ti2 stands out with its enlarged (while not distinctly anisotropic) thermal displacement parameters, namely  $U_{\text{eq}} = 0.022 \text{ Å}^2$ , compared to  $U_{\text{eq}} = 0.014 \text{ Å}^2$  for Ti1 and  $U_{\text{eq}} = 0.010 \text{ Å}^2$  for Ti3. As in the case of the thiospinel, refining the Ti occupancies confirmed the absence of deficiencies, in agreement with the quantitative yields of the reactions starting from the stoichiometric 1:2:4 ratio. Most notably, we refined the occupancy factors of Ti2, the atom with the high displacement parameters, to 1.01(1). In conclusion, the refinements of both CuTi<sub>2</sub>S<sub>4</sub> structures confirmed the absence of deficiencies on any metal sites. Lowering the symmetry by removing the inversion center or the mirror plane did not yield significant changes of the structure model but instead resulted in high correlations. Since the Ti2 atom is the one with the largest Ti–S distances in this structure, it is postulated that the enlarged thermal parameters reflect the rattling effect, caused by matrix effects, as found for the comparable Ti3 atom in Ti<sub>8</sub>Bi<sub>9</sub> (located in a square antiprism)<sup>23</sup> and La in La(Fe/Co)<sub>4</sub>Sb<sub>12</sub> (located in an icosahedron).<sup>24,25</sup>

Crystallographic details for both data collections are compared in Table 1. Atomic positions and isotropic displacement factors for cubic and rhombohedral CuTi<sub>2</sub>S<sub>4</sub> are given in Tables 2 and 3, respectively.

**Electronic Structure Calculations.** Self-consistent tight-binding first principles LMTO calculations (LMTO = linear muffin tin

**Table 3.** Atomic Positions and Isotropic Displacement Factors for Rhombohedral CuTi<sub>2</sub>S<sub>4</sub>

atom	site	x	y	z	$U_{\text{eq}}/\text{Å}^2$
Cu1	6 <i>c</i>	0	0	0.187 59(3)	0.0120(3)
Cu2	6 <i>c</i>	0	0	0.354 49(3)	0.0116(2)
Ti1	3 <i>a</i>	0	0	0	0.0142(5)
Ti2	3 <i>b</i>	0	0		0.0218(5)
Ti3	18 <i>h</i>	0.342 2(1)	0.171 12(6)	0.085 68(3)	0.0101(2)
S1	6 <i>c</i>	0	0	0.123 20(6)	0.0078(4)
S2	6 <i>c</i>	0	0	0.288 92(6)	0.0087(4)
S3	18 <i>h</i>	0.157 02(8)	0.314 0(2)	0.042 34(4)	0.0083(2)
S4	18 <i>h</i>	0.160 20(8)	0.320 4(2)	0.454 37(4)	0.0097(2)

orbitals) were carried out on the primitive cells of both rhombohedral and cubic CuTi<sub>2</sub>S<sub>4</sub>, using the atomic spheres approximation (ASA).<sup>26,27</sup> In the LMTO approach, the density functional theory is used with the local density approximation (LDA).<sup>28</sup> The integration in *k* space was performed by an improved tetrahedron method<sup>29</sup> on a grid of 417 independent *k* points of the first Brillouin zone in the rhombohedral case and 145 *k* points in the case of the cubic thiospinel. The thiospinel is energetically preferred according to the electronic structure calculation, with a lower total energy of 1.6 eV/formula unit. The characters of the different interactions were investigated via the crystal orbital Hamilton population formalism,<sup>30</sup> including calculations of the ICOHP values that are a measure of bond strength.<sup>31</sup>

**Magnetic Susceptibility Measurements.** Variable-temperature magnetization data were collected using a Quantum Design MPMS SQUID magnetometer over the temperature range 2–300 K at an applied field of 500 Oe. Data were taken in both the field-cooled and zero-field-cooled modes. A correction for the core diamagnetism of  $-1.78 \times 10^{-4}$  emu/mol was applied.

## Results and Discussion

**Crystal Structures.** The structure of the rhombohedral modification is shown in Figure 2. The S atoms form densely packed layers that are staggered along the *c* axis in the sequence  $\cdots\text{ABCBCABABCAC}\cdots$ . Overall, the Ti atoms fill half of the octahedral and the Cu atoms one-eighth of the tetrahedral voids of the close-packed S atoms. Two topologically different metal atom layers (surrounded by the S atom layers) alternate along the *c* axis, one comprising both Ti and Cu atoms and one only Ti atoms. This resembles the layer sequences of the spinel (along the [111] direction), wherein the S atom layers are cubic closest-packed (i.e. forming an  $\cdots\text{ABC}\cdots$  sequence). A further distinct difference is the occurrence of Cu–Ti distances of 2.88 Å in the rhombohedral form only, depicted in Figure 2 via dashed lines.

In contrast to the spinel, there are two symmetry-independent metal atom layers in the rhombohedral form that comprise both Ti and Cu atoms, one with Ti1 and Cu2 and the other one with Ti2 and Cu1. As listed in Table 4, they differ significantly in their Ti–S distances, which are  $6 \times 2.41 \text{ Å}$  for each Ti1 and  $6 \times 2.52 \text{ Å}$  for each Ti2, while the

- (22) Sheldrick, G. M. *SHELXTL*, version 5.12 ed.; Siemens Analytical X-ray Systems: Madison, WI, 1995.
- (23) Richter, C. G.; Jeitschko, W. *J. Solid State Chem.* **1997**, *134*, 26–30.
- (24) Braun, D. J.; Jeitschko, W. *J. Less-Common Met.* **1980**, *72*, 147–156.
- (25) Sales, B. C.; Mandrus, D.; Williams, R. K. *Science (Washington, D.C.)* **1996**, *272*, 1325–1328.

- (26) Andersen, O. K. *Phys. Rev.* **1975**, *B12*, 3060–3083.
- (27) Skriver, H. L. *The LMTO Method*; Springer: Berlin, Germany, 1984.
- (28) Hedin, L.; Lundqvist, B. I. *J. Phys.* **1971**, *4C*, 2064–2083.
- (29) Blöchl, P. E.; Jepsen, O.; Andersen, O. K. *Phys. Rev.* **1994**, *B49*, 16223–16233.
- (30) Dronskowski, R.; Blöchl, P. E. *J. Phys. Chem.* **1993**, *97*, 8617–8624.
- (31) Landrum, G. A.; Dronskowski, R. *Angew. Chem., Int. Ed.* **2000**, *39*, 1560–1585.

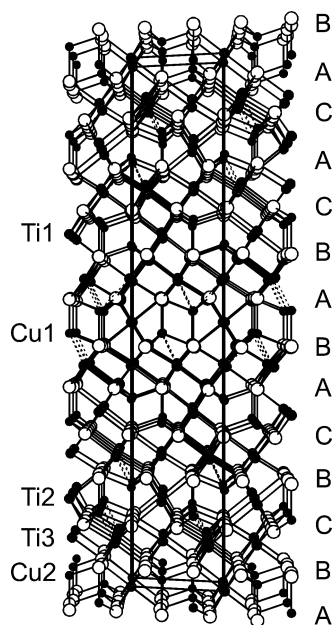


**Figure 2.** Crystal structure of rhombohedral  $\text{CuTi}_2\text{S}_4$  projected along the  $a$  axis (vertical:  $c$  axis). Key: small, black circles, Cu; medium, gray, Ti; large, white, S. The letters A–C denote the packing sequence of the S atoms.

**Table 4.** Selected Interatomic Distances  $d$  (Å) and  $-\text{ICOHP}$  (eV/Bond) Values for Rhombohedral  $\text{CuTi}_2\text{S}_4$

bond	no.	$d$	$-\text{ICOHP}$
Cu1–S1	1×	2.243(2)	2.327
Cu1–S4	3×	2.275(1)	2.254
Cu1–Ti3	3×	2.876(1)	0.437
Cu2–S3	3×	2.268(1)	1.969
Cu2–S2	1×	2.284(2)	1.887
Ti1–S3	6×	2.413(1)	2.362
Ti2–S4	6×	2.515(1)	2.070
Ti3–S4	2×	2.3856(9)	2.498
Ti3–S2	1×	2.442(2)	2.212
Ti3–S1	1×	2.458(1)	2.238
Ti3–S3	2×	2.507(1)	1.924
Ti3–Cu1	1×	2.876(1)	0.437
Ti3–Ti3	2×	3.418(2)	0.185

**Table 5.** Selected Interatomic Distances  $d$  (Å) and  $-\text{ICOHP}$  (eV/Bond) Values for Cubic  $\text{CuTi}_2\text{S}_4$

bond	no.	$d$	$-\text{ICOHP}$
Cu–S	4×	2.2573(7)	2.054
Ti–S	6×	2.4501(4)	2.291
Ti–Ti	6×	3.538(1)	0.132

Cu–S distances are comparable. It is noted that Ti2 is the atom with the enlarged thermal parameters (Table 3). Furthermore, only the Cu1 atom, and not the Cu2 atom, participates in the 2.88 Å contacts to Ti3 (three/Cu1 atom). However, since both of these layers appear virtually equivalent in a projection onto (001) with the surrounding S atoms, we show only one of them in the right part of Figure 3. In each of these layers, the Ti atoms occupy one-quarter of the octahedral, and the Cu atoms one-quarter of the tetrahedral voids of the S atoms. The same description holds for the analogous layer of the cubic form (left part of Figure 3), wherein the Ti–S distances are intermediate to those of the rhombohedral form, namely 2.45 Å (Table 5) compared to 2.41 and 2.52 Å (averaged: 2.46 Å). Moreover, the  $\text{CuS}_4$

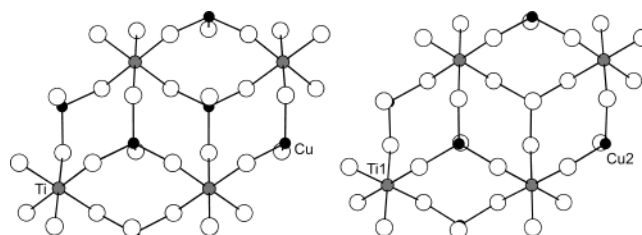


**Figure 3.**  $\text{Ti}_{0.5}\text{CuS}_2$  layers of  $\text{CuTi}_2\text{S}_4$ . Key: small, black circles, Cu; medium, gray, Ti; large, white, S; left, cubic; right, rhombohedral. In the rhombohedral form, the layer comprising Ti2 and Cu1 is topologically equivalent to the one shown with Ti1 and Cu2.

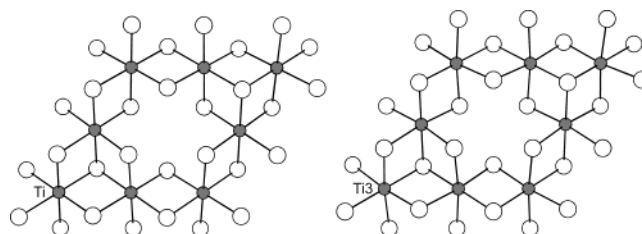


**Figure 4.**  $\text{Ti}_{1.5}\text{S}_2$  layers of  $\text{CuTi}_2\text{S}_4$ . Key: medium, gray, Ti; large, white, S; left, cubic; right, rhombohedral.

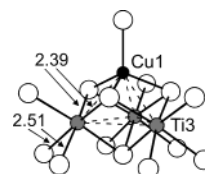


**Figure 5.**  $\text{CuTi}_3\text{S}_{13}$  unit of rhombohedral  $\text{CuTi}_2\text{S}_4$ . Key: small, black circles, Cu; medium, gray, Ti; large, white, S.

tetrahedra are undistorted in the spinel with Cu–S bonds of 2.26 Å (point group of the Cu site:  $\bar{4}3m$ ), and visibly distorted in the rhombohedral form, with bonds between 2.24 and 2.28 Å for Cu1 and 2.27 and 2.28 Å for Cu2 (both averaging to 2.27 Å).

The layers comprising solely Ti atoms are shown in Figure 4 for both modifications. In both cases, the Ti atoms fill three-quarters of the octahedral holes of the S atoms. Again, the S coordination is more regular in case of the spinel (albeit not of full octahedral symmetry), with six 2.45 Å bonds/Ti atom, while the Ti3 atom of rhombohedral  $\text{CuTi}_2\text{S}_4$  comprises four different Ti–S bonds between 2.39 and 2.51 Å, with an average of 2.45 Å.

In the spinel, the Cu atoms cap the triangular faces of the unoccupied  $\text{S}_6$  octahedron of the layer shown in Figure 4. In the rhombohedral form, these voids are capped by one Cu2 and one Ti2 atom, whereas the Cu1 atom caps a tetrahedral void surrounded by three Ti3 atoms, resulting in three Cu1–Ti3 distances of 2.88 Å/Cu1 atom (Figure 5). The Ti3 atoms are shifted toward the Cu1 atom, out of the basal plane of the  $\text{Ti}_3\text{O}_6$  octahedra, as evident by the different Ti3–S distances (2.39 Å vs 2.51 Å). Each of the three Ti3 atoms of Figure 5 exhibits distances of 3.42 Å to the two other Ti3 atoms, which may be a consequence of the shift toward the Cu1 atom. In contrast, the shortest Ti–Ti distance in the spinel is 3.54 Å, appearing six times per Ti atom, and the shortest Cu–Ti distance is 4.15 Å.

This rhombohedral structure of  $\text{CuTi}_2\text{S}_4$  differs quite significantly from other structures obtained by intercalating

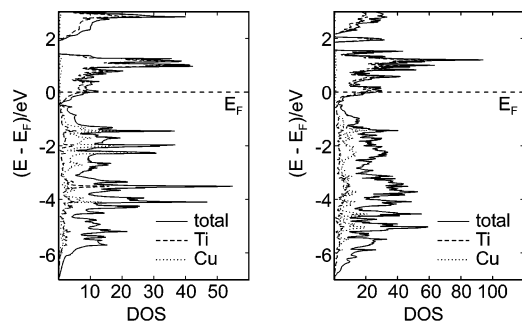


**Figure 6.** Densities of states of  $\text{CuTi}_2\text{S}_4$ . Key: left, cubic; right, rhombohedral. Primitive cell:  $Z = 2$  for cubic and  $Z = 4$  for rhombohedral  $\text{CuTi}_2\text{S}_4$ .

Cu into the  $\text{CdI}_2$  structure of  $\text{TiS}_2$ .<sup>32</sup> In the latter cases, Cu atoms may be added into the van der Waals interlayer region of the  $\text{TiS}_2$  layers while retaining the symmetry, as e.g. shown for  $\text{Cu}_\delta\text{TiS}_2$  with  $\delta = 0.21$  and  $0.38$ .<sup>33</sup> A  $\text{Cu}_{0.7}\text{TiS}_2$  ( $\equiv \text{Cu}_{1.4}\text{Ti}_2\text{S}_4$ )<sup>34</sup> was reported to crystallize in the same space group ( $R\bar{3}m$ ) as the herewith introduced  $\text{CuTi}_2\text{S}_4$ , but it consists of  $\text{TiS}_2$  layers alternating with  $\text{Cu}_{0.7}\text{S}_2$  layers, wherein each tetrahedral void is statistically occupied by 35% Cu. This occurs with a Cu–Ti distance of  $2.72 \text{ \AA}$ .

**Electronic Structure.** The Ti–S averages of  $2.45 \text{ \AA}$  in both  $\text{CuTi}_2\text{S}_4$  modifications are slightly larger than those in  $\text{TiS}_2$  ( $2.43 \text{ \AA}$ )<sup>32</sup> with tetravalent Ti. This may indicate an oxidation state lower than  $4+$  for the Ti atoms, in agreement with the formulation  $\text{Cu}^+(\text{Ti}^{3.5+})_2(\text{S}^{2-})_4$  for the spinel with only one Ti site. The Ti1–S and Ti2–S bonds of the rhombohedral form differ by  $0.11 \text{ \AA}$  in their lengths ( $2.41 \text{ \AA}$  for Ti1;  $2.52 \text{ \AA}$  for Ti2), which is about twice the difference of  $0.06 \text{ \AA}$  between the effective ionic radii of octahedrally coordinated  $\text{Ti}^{3+}$  ( $0.81 \text{ \AA}$ ) and  $\text{Ti}^{4+}$  ( $0.75 \text{ \AA}$ ).<sup>35</sup> While part of the elongation of the Ti2–S bonds, compared to the Ti1–S bonds, stems from the lower oxidation state of Ti2, the elongation is also causing the rattling effect as discussed in the Experimental Section.

With that, one could postulate different oxidation states, namely  $4+$  for Ti1,  $3+$  for Ti2, and  $3.5+$  for Ti3, as the Ti3–S bonds have the same average as the Ti–S bonds in the thiospinel. Taking into consideration the different multiplicities of Ti1, Ti2, and Ti3, one may postulate  $(\text{Cu}^+)_4\text{Ti1}^{4+}\text{Ti2}^{3+}(\text{Ti3}^{3.5+})_6(\text{S}^{2-})_{16}$ .

The calculated densities of states of both  $\text{CuTi}_2\text{S}_4$  modifications (Figure 6) support the assumption of  $\text{Cu}^+$ , as the d states of Cu occur below the Fermi level,  $E_F$ . The Cu contributions around  $E_F$  are approximately zero; the d states of Ti dominate the region between  $-0.5$  and  $3 \text{ eV}$ . Both modifications comprise a significant number of states at  $E_F$ , which are higher per formula unit in case of the rhombohedral form (the DOS are scaled according to the different numbers of formula units). The values are calculated to  $N(E_F) = 76$  states/formula unit for the cubic and  $N(E_F) = 88$  states/

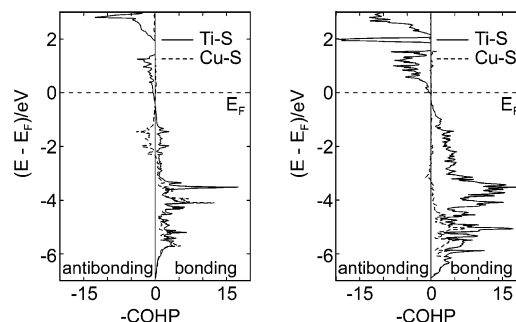


**Figure 7.** Cumulated M–S COHP curves of  $\text{CuTi}_2\text{S}_4$ . Key: left, cubic; right, rhombohedral.

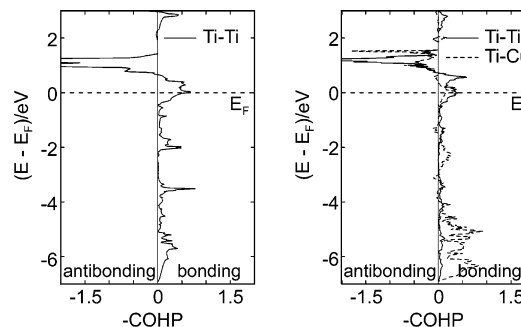


**Figure 8.** Cumulated M–M COHP curves of  $\text{CuTi}_2\text{S}_4$ . Key: left, cubic; right, rhombohedral.

formula unit for the rhombohedral form. The DOS calculated for the cubic form is in agreement with the experimentally determined metallic electrical conductivity of the thiospinel  $\text{CuTi}_2\text{S}_4$ .<sup>19</sup>

The cumulated M–S COHP curves are shown in Figure 7. In both cases, the Ti–S bonds are optimized, i.e., the first antibonding states become filled just around  $E_F$ . On the other hand, some antibonding Cu–S states are filled in case of the cubic modification but not in the rhombohedral form, where the Cu–S bonds are optimized as well. Correspondingly, the averaged absolute Cu–S ICOHP values are larger in the rhombohedral form ( $-2.11 \text{ eV/bond}$ , compared to  $-2.05 \text{ eV/bond}$  in the thiospinel), which indicates stronger bonding. On the other hand, the Ti–S bonds are on average weaker in the rhombohedral form ( $-2.22 \text{ eV}$  vs  $-2.29 \text{ eV}$ ).

Last, we turn our attention toward the metal–metal interactions. Only in the rhombohedral form do Cu–Ti contacts ( $<4 \text{ \AA}$ ) occur, with a length of  $2.88 \text{ \AA}$ . As well, the shortest Ti–Ti distances are found in the rhombohedral form ( $3.42 \text{ \AA}$  vs  $3.54 \text{ \AA}$  in the spinel), while the multitude of these distances is higher in the spinel, namely  $6 \times / \text{Ti}$ , compared to  $2 \times / \text{Ti3}$  in the rhombohedral form. The respective COHP curves (Figure 8) reveal that all of these interactions have bonding character, with virtually no antibonding states filled. The ICOHP values ( $-0.44$  for the Cu–Ti bond and  $-0.19$  and  $-0.13 \text{ eV/bond}$  for the shortest Ti–Ti bonds of the rhombohedral and cubic form, respectively) point toward medium to weak bonding character. Much higher ICOHP values were found for the intermediate Ti–Ti bonds of  $3.35$  and  $3.40 \text{ \AA}$  in  $\text{Ti}_2\text{Sb}$  with  $-0.64$  and  $-0.75 \text{ eV/bond}$  because of the lower oxidation states of the Ti atoms in  $\text{Ti}_2\text{Sb}$ .<sup>36</sup>

(32) Furuseth, S. J. *Alloys Compd.* **1992**, *178*, 211–215.

(33) Kusawake, T.; Takahashi, Y.; Ohshima, K.-I. *Mol. Cryst. Liq. Cryst.* **2000**, *341*, 93–98.

(34) le Nagard, N.; Gorochoy, O.; Collin, G. *Mater. Res. Bull.* **1974**, *10*, 1287–1296.

(35) Shannon, R. D. *Acta Crystallogr.* **1976**, *A32*, 751–767.

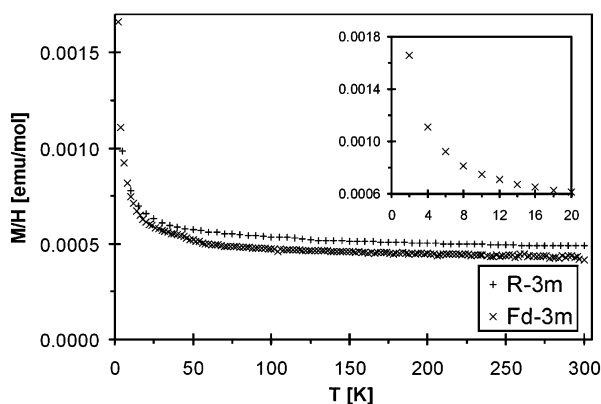


**Figure 9.** Magnetic susceptibilities of  $\text{CuTi}_2\text{S}_4$ . Key:  $\times$ , cubic;  $+$ , rhombohedral. The inset displays the low-temperature region of the cubic modification.

Increasing the valence-electron concentration in either case would further strengthen the bonds by filling more bonding states.

**Physical Properties.** The electronic structure calculations predict metallic properties, e.g. metallic conductivity and Pauli paramagnetism, for both modifications. The magnetic susceptibilities of both modifications of  $\text{CuTi}_2\text{S}_4$ , corrected for the diamagnetic contributions, are compared in Figure 9. Both data sets are consistent with Pauli paramagnetism and a small Curie–Weiss paramagnetic impurity. Thus, the data were fitted according to  $\chi = C/(T - \Theta) + \chi_{\text{TIP}}$ , with  $\chi$  = magnetic susceptibility,  $C$  = Curie constant,  $T$  = temperature,  $\Theta$  = critical temperature, and TIP = temperature independent (Pauli) paramagnetism. We obtained for the rhombohedral modification  $C = 5.4(2) \times 10^{-3}$  emu/mol (spinel: 4.9(1)),  $\Theta = -7.0(8)$  K (spinel:  $-3.3(3)$ ), and  $\chi_{\text{TIP}} = 4.80(2) \times 10^{-4}$  emu/mol (spinel: 4.20(1)). In both cases, the observed Curie constants are  $\approx 1\%$  of that expected for a single spin (0.375 emu/mol). The higher value of the TIP in case of the rhombohedral form correlates nicely with its higher densities of states at  $E_{\text{F}}$ . In fact, the ratio  $\chi_{\text{TIP}}(R\bar{3}m)/$

$\chi_{\text{TIP}}(Fd\bar{3}m) = 1.14$  is in quantitative agreement with the calculated ratio  $N(E_{\text{F}})(R\bar{3}m)/N(E_{\text{F}})(Fd\bar{3}m) = 1.16$ .

The TIP value of the spinel is comparable to the TIP of  $4.26 \times 10^{-4}$  emu/mol measured in 2000.<sup>19</sup> On the other hand, neither the postulated halfmetallic ferromagnetic ground state<sup>17</sup> nor the spin gap extrapolated from NMR experiments at 5 K<sup>18</sup> was confirmed, as the inset of Figure 9 shows. Note, however, that a transition to the ferromagnetic state might occur below the temperature range investigated (2–300 K).

## Conclusion

A new, rhombohedral modification of  $\text{CuTi}_2\text{S}_4$  was uncovered via a flux method, which is likely the kinetically preferred variant, compared to the known cubic thiospinel. Alternatively, the rhombohedral form may be prepared directly from the elements without the addition of a flux at 425 °C. Compared to the cubic form, the rhombohedral one comprises stronger Cu–Ti and Cu–S bonds but weaker Ti–S bonds. Furthermore, all Ti sites in the spinel are symmetry equivalent, while three different Ti sites occur in the rhombohedral modification. That their distances to the S atoms differ by up to 0.11 Å is a hint toward mixed valence of the Ti atoms. Both modifications are metallic exhibiting Pauli paramagnetism, which is larger in case of the rhombohedral form, in quantitative agreement with the calculated densities of states.

**Acknowledgment.** Financial support from the NSERC, CFI, OIT (Ontario Distinguished Researcher Award for H.K.), the Province of Ontario (Premier’s Research Excellence Award for H.K.), and the Canada Research Chair program (CRC for H.K.) is appreciated. We thank Dr. P. Dube and Ms. A. Sefat for assistance with the SQUID magnetometer measurements at the Brockhouse Institute for Materials Research at McMaster University.

**Supporting Information Available:** Two X-ray crystallographic files in CIF format and two figures displaying the  $H/M$  vs  $T$  fits. This material is available free of charge via the Internet at <http://pubs.acs.org>.

IC0495113

(36) Derakhshan, S.; Assoud, A.; Kleinke, K. M.; Dashjav, E.; Qiu, X.; Billinge, S. J. L.; Kleinke, H. *J. Am. Chem. Soc.* **2004**, *126*, 8295–8302.